POLITECNICO DI TORINO
Repository ISTITUZIONALE

Functional Design and Kinematic Analysis of a Novel 3RS End-Effector Robot for Wrist Rehabilitation and Assistance

Original
Functional Design and Kinematic Analysis of a Novel 3RS End-Effector Robot for Wrist Rehabilitation and Assistance / Botta, A., Tagliavini, L., Colucci, G., Baglieri, L., Duretto, S., Toccaceli, L., Amodio, F., Quaglia, G.. - ELETTRONICO. - 190:(2025), pp. 268-277. (34th International Conference on Robotics in Alpe-Adria-Danube Region (RAAD 2025) Belgrade (SRB) 18 - 20 June, 2025) [10.1007/978-3-032-02106-9_30].

Availability:
This version is available at: 11583/3002747 since: 2025-09-03T08:24:31Z

Publisher:
Springer

Published
DOI:10.1007/978-3-032-02106-9_30

Terms of use:

This article is made available under terms and conditions as specified in the corresponding bibliographic description in the repository

Publisher copyright
Springer postprint/Author's Accepted Manuscript

This version of the article has been accepted for publication, after peer review (when applicable) and is subject to Springer Nature's AM terms of use, but is not the Version of Record and does not reflect post-acceptance improvements, or any corrections. The Version of Record is available online at: http://dx.doi.org/10.1007/978-3-032-02106-9_30

(Article begins on next page)

29 November 2026

Functional Design and Kinematic Analysis of a Novel 3RS End-Effector Robot for Wrist Rehabilitation and Assistance

Andrea Botta, Luigi Tagliavini, Giovanni Colucci, Lorenzo Baglieri, Simone Duretto, Lorenzo Toccaceli, Francesco Amodio, and Giuseppe Quaglia

DIMEAS Department of Mechanical and Aerospace Engineering, Politecnico di Torino, Corso Duca degli Abruzzi 24, 10129 Torino, Italy
andrea.botta@polito.it

Abstract. Robot-aided rehabilitation is increasingly important to meet the challenges posed by an ageing population and a global shortage of healthcare workers. This paper presents a 3RS (3 Revolute Joints - 1 Spherical Joint) end-effector robot for wrist joint rehabilitation and daily activity assistance. It assists flexion/extension and radial/ulnar deviation avoiding the problem of joint misalignment typical of exoskeletons and covering the workspace of the hand. The design parameters are tuned to ensure high dexterity and safe user interaction, laying a solid foundation for the development of a functional prototype.

Keywords: robot-assisted rehabilitation, assistive technology, end-effector robot.

1 Introduction

Robot-aided rehabilitation and assistive technologies are becoming essential as the global population ages, the incidence of disabilities increases, and the lack of medical personnel worsens. According to the World Health Organization (WHO) [1], 1.3 billion people worldwide experience significant disability. The global population of 60 years and older is projected to reach 2.1 billion by 2050 [2], further increasing the prevalence of age-related conditions requiring rehabilitation. These trends and the global shortage of medical professionals highlight the need for effective rehabilitation solutions to enhance recovery and improve daily activities.

Albanese *et al.* reported on the effectiveness of robot-aided orthopedic rehabilitation and how it is comparable to traditional treatments, potentially reducing human therapists' effort and increasing subject engagement and voluntary participation [3]. This demonstrates robotics solutions play a critical role in providing therapy and enabling telemedicine options that are particularly beneficial in regions with limited access to healthcare and welfare.

Hussain *et al.* classified rehabilitation robots into two types: exoskeletons and end-effectors [4].

– Exoskeleton-type robots mimic the user's kinematic chain and are ideal for wearable devices that control multiple joints. However, they require precise alignment to avoid unintended forces and potential joint damage.
– End-effector robots connect to the user at a single point. This eliminates alignment issues but complicates the accurate application of forces and torques due to the lack of correspondence between the robot's and human's joints.

The literature presents examples of both exoskeleton and end-effector robots, with some devices blending the two classifications. Gonçalves *et al.* created a desk-based end-effector robot with a single degree of freedom (DOF) that performs two wrist motions through setup adjustments [5]. Shi *et al.* developed a cable-driven 3-DOF robot, though it is non-portable due to its bulky actuation system [6]. In contrast, the authors developed a cable-driven solution for active or passive rehabilitation, portable and lightweight [7, 8]. Buongiorno *et al.* designed a 3-DOF exoskeleton that integrates with a 7-DOF arm and hand exoskeleton [9]. Higuma *et al.* presented a lightweight, portable 2-DOF exoskeleton that uses compliance to address joint misalignment issues [10]. Table 1 collects some selected wrist rehabilitation devices and compares their main features.

Table 1: Features of a selection wrist rehabilitation devices

Device	**Type**	**Portable**	**DOF**	**Note**
[5]	End-effector	Fixed	1 - FE or RUD	Change setup to change desired motion
[6]	End-effector	Fixed	3 - FE, RUD, PS	Cable-driven
[7, 8]	End-effector	Portable	3 - FE, RUD, PS	Cable-driven
[9]	Exoskeleton	Portable	3 - FE, RUD, PS	Integrated in an upper arm exoskeleton
[10]	Exoskeleton	Portable	2 - FE, RUD	Adds compliance to avoid joint misalignment
[11]	Exoskeleton	Fixed	3 - FE, RUD, PS	
[12]	Exoskeleton	Fixed	3 - FE, RUD, PS	
[13]	Exoskeleton	Fixed	3 - FE, RUD, PS	Adds compliance to avoid joint misalignment
[14]	Exoskeleton	Fixed	3 - FE, RUD, PS	
[15]	Exoskeleton	Fixed	3 - FE, RUD, PS	
[16, 17]	Exoskeleton	Portable	3 - FE, RUD, PS	
[18]	End-effector	Portable	3 - FE, RUD, PS	Pneumatic muscles
3RS	End-effector	Portable	2 - FE, RUD	Bowden cables

FE - Flexion/Extension, RUD - Radial/Ulnar Deviation, PS - Pronation/Supination (forearm rotation), 3RS - 3 Revolute Joints 1 Spherical Joint

The literature highlights a lack of lightweight, wearable, and portable wrist rehabilitation robots. Moreover, most of the portable solutions are exoskeletons, requiring additional compensation mechanisms to overcome joint misalignments.

To address this issue, we introduce a new 3RS (3 Revolute Joints - 1 Spherical Joint) end-effector-type robot designed for wrist joint rehabilitation and assistance. This robot can either guide the user's hand through pre-recorded motions (active mode) or provide controlled resistance to the user's movements (passive mode). The robot should be able to assist the two wrist motions: the flexion/extension (FE, α) and the radial/ulnar deviation (RUD, β). To simplify its design, forearm pronation/supination is neglected by fixing the robot frame close enough to the wrist joint.

2 Proposed Design

The wrist joint is quite complex, and the two aforementioned motions are far from simple rotations about fixed axes. Therefore, using an end-effector solution that contains the hand's workspace is simpler than developing an exoskeleton that mimics the human wrist joint and includes mechanisms to prevent joint misalignment that could harm the user.

The robot is intended to be worn around the distal end of the forearm close to the wrist to ensure its frame is consistent with the pronation and supination motions of the entire forearm. To enhance wearability and portability for extended use, while also optimizing weight distribution, the robot's joints are actuated remotely via Bowden cables arranged in a tendon-like configuration and driven from the user's back or upper arm [19]. Additionally, most of the electronic power and control subsystems should be placed near the actuators to minimize weight on the forearm.

Figure 1 displays the proposed 3RS kinematic chain to aid the user's hand movements. As the name suggests, the first three joints, namely J_1, J_2, and J_3, are revolute joints. The joint J_1 is fixed to the distal end of the forearm just behind the ideal wrist centre $\{0\}$ by means of a wristband. The last one, J_4, is a spherical joint that links the robot to the hand. In practice, J_4 is fixed to the back of the hand. However, for simplicity in solving robot inverse kinematics, this joint is placed on the coronal plane of the hand.

The first two joints J_1 and J_2 are designed to be driven by tendon-like pulleys to enable remote control of the two Degrees of Freedom (DOF). Joints J_3 and J_4 are instead passive. In particular, it can be shown that J_1 and its rotation q_1 are directly related to the hand FE motion α, as shown by the side view in Fig. 1b. Similarly, Fig. 1c illustrates from a top view how the rotation q_2 of joint J_2 controls the RUD angle β.

The proposed solution has to be sensorized to properly control the robot while always guaranteeing the safety of its user. FE α and RUD β can be obtained by computing the relative orientation between the hand and the forearm (the frame of the mechanism). This could be achieved by employing two IMUs (Inertial Measurement Units), one fixed to the robot frame and the other integral to the hand interface. Moreover, joints J_1, J_2, and J_3 will be sensorized to measure their respective angles. By using all this data, it should be possible to continuously monitor the hand and robot kinematics to avoid the occurrence

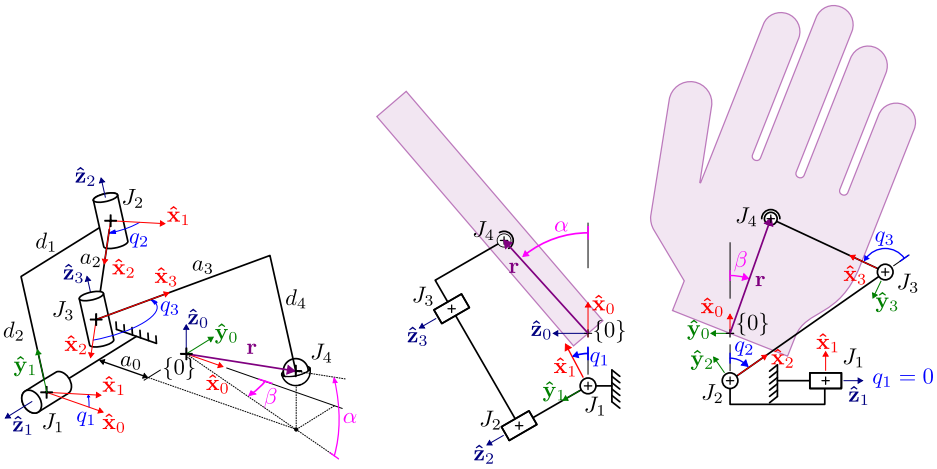


Fig. 1: Different view of the functional diagram of the proposed 3RS robot. (a) 3D view with complete nomenclature. (b) Side-view with focus on flexion/extension. (c) Top-view with focus on radial/ulnar deviation.

of unsafe configurations. The same setup could also be handy to calibrate the device to each individual based on his/her preferences and mobility limit. For example, the user may define the desired range of motion while wearing the device for the first time by moving his/her hand freely while being tracked by the device sensors. The robot will be controlled to avoid going beyond such limits. At last, mechanical stops could be added to prevent undesired motions.

In parallel to the purely kinematic control, it's also critical to guarantee that forces and torques applied by the device are controlled. To this end, the actuation of joints J_1 and J_2 should implement a torque feedback together with the position one. On this topic, the solution proposed in [19], i.e., using Series Elastic Actuators (SEA), seems very promising. Although the introduction of an elastic element in the transmission affects the high-frequency dynamics of the actuator, it should be possible to design more precise torque controllers with the added benefit of compliance and low mechanical impedance.

3 Robot Kinematics

The robot's direct kinematics can be easily derived using the composition of transformation resulting from the Denavit–Hartenberg (DH) parameters, such as

$$ {}^{i-1}\mathbf{T}_i = \mathrm{Rot}_{\hat{\mathbf{x}}_{i-1}}(\alpha_{i-1}) \cdot \mathrm{Trans}_{\hat{\mathbf{x}}_{i-1}}(a_{i-1}) \cdot \mathrm{Rot}_{\hat{\mathbf{z}}_i}(\theta_i) \cdot \mathrm{Trans}_{\hat{\mathbf{x}}_i}(d_i); \qquad (1) $$

where

– ${}^{i-1}\mathbf{T}_i$ is the homogeneous transformation from J_{i-1} to J_i

- α_{i-1}: offset angle measured from $\hat{\mathbf{z}}_{i-1}$ to $\hat{\mathbf{z}}_i$ about $\hat{\mathbf{x}}_{i-1}$;
- a_{i-1}: link length measured from $\hat{\mathbf{z}}_{i-1}$ to $\hat{\mathbf{z}}_i$ about $\hat{\mathbf{x}}_{i-1}$;
- d_i: link offset measured from $\hat{\mathbf{x}}_{i-1}$ to $\hat{\mathbf{x}}_i$ about $\hat{\mathbf{z}}_i$;
- θ_i: joint angle measured from $\hat{\mathbf{x}}_{i-1}$ to $\hat{\mathbf{x}}_i$ about $\hat{\mathbf{z}}_i$;

In particular, the modified DH parameters are used because they are more straightforward to apply to this case. Table 2 collects all parameters.

Table 2: List of modified DH parameters

Joint i	α_{i-1}	a_{i-1}	d_i	θ_i	Note
J_1	$\pi/2$	$-a_0$	d_1	q_1	from 0 to J_1
J_{11}	0	0	$-d_1$	0	Virtual joint below J_2 along $\hat{\mathbf{z}}_2$
J_2	$-\pi/2$	0	d_2	q_2	from J_{11} to J_2
J_3	0	a_2	0	q_3	from J_2 to J_3
J_4	0	a_3	$-d_4 = -d_2$	0	from J_3 to J_4

Regarding the inverse kinematics, given a desired hand orientation defined by the angles α and β and the fixed distance $r = |\mathbf{r}|$ it is possible to define the corresponding Cartesian coordinates of J_4 as

$$x = r\cos(\alpha)\cos(\beta), \qquad y = r\cos(\alpha)\sin(\beta), \qquad z = r\sin(\alpha). \tag{2}$$

Referring to Fig. 2, it can be shown that the rotation q_1 of joint J_1 is only directly related to the flexion-extension angle α, that is

$$q_1 = \arctan\left(\frac{z}{x + a_0}\right). \tag{3}$$

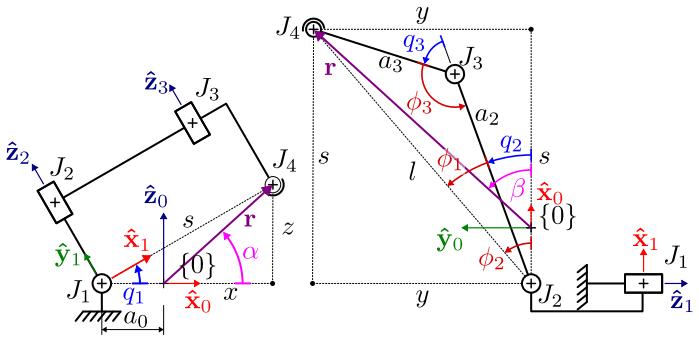


Fig. 2: Different views of the robot to define quantities useful to solve the inverse kinematics. On the left side view showing a FE motion, on the right a top view with a RUD motion.

Before solving for q_2 and q_3, it is useful defining some auxiliary geometric quantities, such as

$$s = \sqrt{(x + a_0)^2 + z^2}, \qquad l = \sqrt{s^2 + y^2},$$

$$\phi_1 = \arccos\left(\frac{a_2^2 + l^2 - a_3^2}{2a_2 l}\right), \quad \phi_2 = \arctan\left(\frac{y}{s}\right), \quad \phi_3 = \arccos\left(\frac{a_2^2 + a_3^2 - l^2}{2a_2 a_3}\right);$$

so that

$$q_2 = \phi_2 - \phi_1; \tag{4}$$

$$q_3 = \pi - \phi_3. \tag{5}$$

One key feature of end-effector rehabilitation devices is that they don't need to mimic the kinematic chain of the articulation. On the contrary, it is sufficient that the robot's workspace include the hand's workspace to behave properly. Then, a controller based on the inverse kinematics and the human wrist range of motion guarantees that the robot performs only movements that are feasible for the wrist joint.

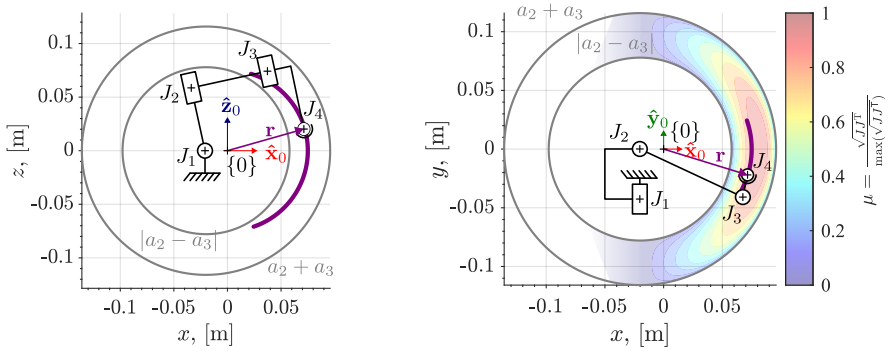
Table 3 collects an average of motion range data, based on a comprehensive review of relevant literature sources [20, 21], encompassing both the maximum feasible range of motion and the range necessary for activities of daily living (ADLs). While a healthy joint could achieve the full range of motion, rehabilitation practices aim to recover the joint in order to achieve at least the mobility required for daily tasks. Using the simplest model considering the wrist a universal joint, the hand workspace is a sphere cap with radius $\mathbf{r}$ and angular extension equal to the maximum range of motion. The literature indicates that the average palm length, measured from the ideal wrist centre to the base of the fingers for both male and female populations, is $99.7 \pm 8.1\,\text{mm}$ [22]. Thus, a radius $|\mathbf{r}| = 75\,\text{mm}$ is considered to connect the robot close to the back of the hand centre using a glove or something equivalent.

Table 3: Wrist joint maximum and ADLs ranges of motions

Motion	**Max Range**	**ADL Range**
α, FE extension (−) flexion (+)	$[-71°, 73°]$	$[-54°, 60°]$
β, RUD ulnar (−) radial (+)	$[-33°, 19°]$	$[-33°, 19°]$

The proposed robot's workspace is a portion of a spherical shell with an inner radius equal to $|a_2 - a_3|$ and an outer radius of $a_2 + a_3$ and centred in $J_{11} = [-a_0, 0, 0]^\mathsf{T}$. With the correct sizing of the robot, if the robot's workspace encloses the hand's workspace, it is possible to safely assist the hand motion without causing any harm due to joint misalignment. Figure 3 compares the two workspaces for both wrist motions.

Furthermore, Fig. 3b illustrates the normalized manipulability index $\mu = \sqrt{J_t J_t^\mathsf{T}}$, where J_t represents the linear component of the robot's Jacobian matrix.



(a) (b)

Fig. 3: 3RS robot's workspace and hand workspace (purple). (a) Flexion/extension motion. (b) Radial/ulnar deviation motion with manipulability index

A higher value of μ indicates greater dexterity of the robot at a given point. Notably, the figure shows that μ approaches zero near the edges of the workspace due to the robot reaching singular configurations. Conversely, the maximum value of μ occurs at $k \approx 80 \div 85\%$ of the external radius $a_2 + a_3$. Therefore, to ensure good dexterity near the hand path, the following condition must be satisfied:

$$k(a_2 + a_3) \approx r + a_0 \tag{6}$$

The relationship is not an exact constraint, as the actual motion of the hand does not follow a perfect arc centred in $\{O\}$. Instead, it follows a more complex trajectory with no single, fixed centre of rotation. Thus, in the following, k will be equal to 82% as an average between the threshold values.

It can also be demonstrated that for both motions, as J_1 approaches O, i.e. as a_0 decreases to 0, the instantaneous transmission ratio tends toward 1. Additionally, larger value of r further reduce the transmission ratio. However, achieving a transmission ratio lower than 1 requires placing the joint J_1 of O. Unfortunately, this configuration is undesirable as it may cause frequent interference with the hand movements or the surrounding environment. Considering these factors, a value of $a_0 = 20\,\text{mm}$ has been selected as practical trade-off to still be very close to 0 but leaving enough room for the physical joint and its actuation.

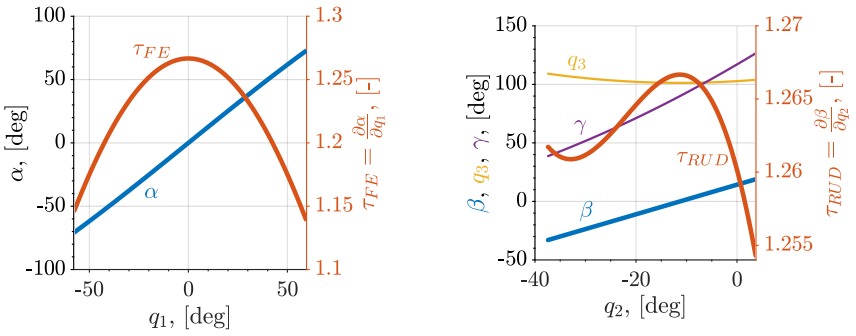
The dimensions a_2 and a_3 do not influence the transmission ratio but can be optimized to improve the transmission angle of the mechanism by ensuring that link a_3 is as perpendicular as possible to both r and a_2. This configuration is achieved using the following relationship

$$a_2^2 = a_3^2 + (r + a_0)^2 \tag{7}$$

this ensures that a_3 is perpendicular to r when $\beta = 0°$ and remains nearly perpendicular during motion. The equation assumes that $a2 > r + a0 > 0$.

Using Eqs.(6) and (7) and the previously chosen values $r = 75\,\text{mm}$, $a_0 = 20\,\text{mm}$, and $k = 82\%$ the calculated parameters are $a_2 = 97\,\text{mm}$ and $a_3 = 19\,\text{mm}$. The parameters d_1, d_2, and d_4 are not significant for the transmission ratio and depend only on the dimensions of the forearm and hand. They have been set to 65 mm, 60 mm, and 60 mm, respectively.

The proposed dimensions results in the kinematic characteristics illustrated in Fig. 4. For flexion/extension motion, there is an approximately linear relation between q_1 and α with an instantaneous transmission ratio $\tau_{FE} = \partial\alpha/\partial q_1 = 1.123 \pm 0.037$. A similar behaviour is observed for radial/ulnar deviation, where $\beta(q_2)$ is nearly linear with minimal oscillations, yielding an istantaneous transmission ratio $\tau_{RUD} = \partial\beta/\partial q_2 = 1.26 \pm 0.003$. For this motion, the angle q_3 and $\gamma = q_2 + q_3 + \beta$, which is angle between a_3 and $\mathbf{r}$ are also shown. The angle q_3 remains nearly constant and close to 90° providing good force transmission, while γ approaches 90° primarily around the resting position $\beta = 0°$.



(a) (b)

Fig. 4: 3RS robot's kinematic behaviour showing both the relation between joint angles and wrist angles and the respective instantaneous transmission ratios. (a) Flexion/extension. (b) Radial/ulnar deviation.

It's worth noting that the device workspace abundantly includes the hand one. This means that not only this device can compensate for the natural deviation from the simplified assumption of the wrist acting as an ideal universal joint, but it can also compensate for different user and their anatomy. Obviously, this possibility would be sub-optimal in terms of performance and generally not suggested. The intended approach would be to design custom-made devices for each user, that is, sizing the device links based on the user anatomy following the guidelines presented in this work. An alternative approach would be making adjustable link lengths to adapt the device to its user.

4 Conclusions

This paper introduces a design and analysis of a 3RS end effector robot, for wrist rehabilitation purposes. The mechanism aims to provide an optimized work area and constant transmission ratio to assist wrist movements effectively and enhance dexterity, in flexion/extension as in radial/ulnar deviation motions of the wrist. The proposed design shows potential, in improving rehabilitation methods and facilitating the incorporation of robotic technology into assistive healthcare devices. This positive outcome will lead to the development of a prototype where the first two robot joints are remotely driven by a tendon-actuated configuration to reduce the device weight close to the wrist.

References

1. World Health Organization: Health equity for persons with disabilities: guide for action: executive summary (Jan 2025), https://www.who.int/publications/i/item/B09201, accessed: 2025-01-15
2. World Health Organization: Ageing and health (Oct 2024), https://www.who.int/news-room/fact-sheets/detail/ageing-and-health, accessed: 2025-01-15
3. Albanese, G.A., Taglione, E., Gasparini, C., Grandi, S., Pettinelli, F., Sardelli, C., Catitti, P., Sandini, G., Masia, L., Zenzeri, J.: Efficacy of wrist robot-aided orthopedic rehabilitation: a randomized controlled trial. Journal of NeuroEngineering and Rehabilitation 18(1), 130 (Aug 2021), https://doi.org/10.1186/s12984-021-00925-0
4. Hussain, S., Jamwal, P.K., Van Vliet, P., Ghayesh, M.H.: State-of-the-Art Robotic Devices for Wrist Rehabilitation: Design and Control Aspects. IEEE Transactions on Human-Machine Systems 50(5), 361–372 (Oct 2020), conference Name: IEEE Transactions on Human-Machine Systems
5. Gonçalves, R.S., Brito, L.S.F., Moraes, L.P., Carbone, G., Ceccarelli, M.: A fairly simple mechatronic device for training human wrist motion. International Journal of Advanced Robotic Systems 17(6), 1729881420974286 (Nov 2020), https://doi.org/10.1177/1729881420974286, publisher: SAGE Publications Sage UK: London, England
6. Shi, K., Song, A., Li, Y., Li, H., Chen, D., Zhu, L.: A Cable-Driven Three-DOF Wrist Rehabilitation Exoskeleton With Improved Performance. Frontiers in Neurorobotics 15 (2021), https://www.frontiersin.org/article/10.3389/fnbot.2021.664062
7. Botta, A., Quaglia, G., Takeda, Y.: Wearable Passive Cable-Driven Wrist Rehabilitation Robot: Design and Preliminary Experiments. In: Okada, M. (ed.) Advances in Mechanism and Machine Science. pp. 103–112. Mechanisms and Machine Science, Springer Nature Switzerland, Cham (2023)
8. Quaglia, G., Botta, A., Colucci, G., Takeda, Y.: RehaWrist.q - Development of a 3 DoF Cable-Driven End-Effector Wearable Robot for Rehabilitation of the Wrist Joint. In: Petuya, V., Quaglia, G., Parikyan, T., Carbone, G. (eds.) Proceedings of I4SDG Workshop 2023. pp. 136–145. Mechanisms and Machine Science, Springer Nature Switzerland, Cham (2023)
9. Buongiorno, D., Sotgiu, E., Leonardis, D., Marcheschi, S., Solazzi, M., Frisoli, A.: WRES: A Novel 3 DoF WRist ExoSkeleton With Tendon-Driven Differential Transmission for Neuro-Rehabilitation and Teleoperation. IEEE Robotics and Automation Letters 3(3), 2152–2159 (Jul 2018), conference Name: IEEE Robotics and Automation Letters

10. Higuma, T., Kiguchi, K., Arata, J.: Low-Profile Two-Degree-of-Freedom Wrist Exoskeleton Device Using Multiple Spring Blades. IEEE Robotics and Automation Letters 3(1), 305–311 (Jan 2018), conference Name: IEEE Robotics and Automation Letters
11. Martinez, J.A., Ng, P., Lu, S., Campagna, M.S., Celik, O.: Design of Wrist Gimbal: A forearm and wrist exoskeleton for stroke rehabilitation. In: 2013 IEEE 13th International Conference on Rehabilitation Robotics (ICORR). pp. 1–6 (Jun 2013), iSSN: 1945-7901
12. Pehlivan, A.U., Sergi, F., Erwin, A., Yozbatiran, N., Francisco, G.E., O'Malley, M.K.: Design and validation of the RiceWrist-S exoskeleton for robotic rehabilitation after incomplete spinal cord injury. Robotica 32(8), 1415–1431 (Dec 2014), https://www.cambridge.org/core/journals/robotica/article/design-and-validation-of-the-ricewrists-exoskeleton-for-robotic-rehabilitation-after-incomplete-spinal-cord-injury/B804AEF7C4428AB7B291CE9FB2A18574, publisher: Cambridge University Press
13. Omarkulov, N., Telegenov, K., Zeinullin, M., Tursynbek, I., Shintemirov, A.: Preliminary mechanical design of NU-Wrist: A 3-DOF self-aligning Wrist rehabilitation robot. In: 2016 6th IEEE International Conference on Biomedical Robotics and Biomechatronics (BioRob). pp. 962–967 (Jun 2016), iSSN: 2155-1782
14. Pezent, E., Rose, C.G., Deshpande, A.D., O'Malley, M.K.: Design and characterization of the OpenWrist: A robotic wrist exoskeleton for coordinated hand-wrist rehabilitation. In: 2017 International Conference on Rehabilitation Robotics (ICORR). pp. 720–725 (Jul 2017), iSSN: 1945-7901
15. Akdoğan, E., Aktan, M.E., Koru, A.T., Selçuk Arslan, M., Atlıhan, M., Kuran, B.: Hybrid impedance control of a robot manipulator for wrist and forearm rehabilitation: Performance analysis and clinical results. Mechatronics 49, 77–91 (Feb 2018), https://www.sciencedirect.com/science/article/pii/S0957415817301782
16. Su, Y.Y., Wu, K.Y., Lin, C.H., Yu, Y.L., Lan, C.C.: Design of a Lightweight Forearm Exoskeleton for Fine-Motion Rehabilitation. In: 2018 IEEE/ASME International Conference on Advanced Intelligent Mechatronics (AIM). pp. 438–443 (Jul 2018), iSSN: 2159-6255
17. Su, Y.Y., Yu, Y.L., Lin, C.H., Lan, C.C.: A compact wrist rehabilitation robot with accurate force/stiffness control and misalignment adaptation. International Journal of Intelligent Robotics and Applications 3(1), 45–58 (Mar 2019), https://doi.org/10.1007/s41315-019-00083-6
18. Hussain, S., Jamwal, P.K., Van Vliet, P.: Design synthesis and optimization of a 4-SPS intrinsically compliant parallel wrist rehabilitation robotic orthosis. Journal of Computational Design and Engineering 8(6), 1562–1575 (Dec 2021), https://doi.org/10.1093/jcde/qwab061
19. Botta, A., Tagliavini, L., Colucci, G., Baglieri, L., Duretto, S., Takeda, Y., Quaglia, G.: Compact Series Elastic Actuator for a Wrist Exoskeleton for Daily Living Assistance. In: Quaglia, G., Boschetti, G., Carbone, G. (eds.) Advances in Italian Mechanism Science. pp. 76–83. Springer Nature Switzerland, Cham (2024)
20. Neumann, D.A.: Kinesiology of the Musculoskeletal System - Foundations for Rehabilitation. Elsevier Health Sciences, 3 edn. (Nov 2016)
21. Ryu, J., Cooney, W.P., Askew, L.J., An, K.N., Chao, E.Y.S.: Functional ranges of motion of the wrist joint. The Journal of Hand Surgery 16(3), 409–419 (May 1991), https://www.sciencedirect.com/science/article/pii/036350239190006W
22. Rai, A., Pawar, P., Khandelwal, M., Parkar, S., Patel, U.: The study of correlation between palm length, palm width and hand length with stature in the students. IP International Journal of Forensic Medicine and Toxicological Sciences 8(4), 148–153 (2023), https://www.ijfmts.com/article-details/20792